Corrosion characterization of tin-lead and lead free solders in 3.5wt.% NaCl solution

Dezhi Li*, Paul P. Conway, Changqing Liu

Wolfson School of Mechanical and Manufacturing Engineering

Loughborough University, Loughborough, Leicestershire, LE11 3TU, UK

*Corresponding author: E-mail: D.Li@lboro.ac.uk

Tel: +44 (0)1509 227568

Fax: +44 (0)1509 227549

Abstract

The corrosion resistance of Sn-Pb and several candidate lead free solders were investigated in 3.5wt.% NaCl solution through potentiodynamic polarisation. Results showed that in NaCl solution lead free solders had better corrosion resistance than Sn-Pb solder and the corrosion resistance of lead free solders was similar, but the corrosion resistance of Sn-Ag solder was better than that of Sn-Ag-Cu and Sn-Cu solders. The corrosion products for Sn-Pb solder had a two-layered structure with Sn-rich phases at the outer layer and looser Pb-rich phases at the inner layer. The loose Pb-rich layer was detrimental to the corrosion property. The corrosion product on the surface of all these solders was tin oxide chloride hydroxide.

Keywords: A. Eutectic Sn-Pb solder; A. Lead free solders; B. potentiodynamic polarisation; C. passivation film

1. Introduction

Sn-Pb solders have been widely used in electronic industries due to their low cost, good solderability, low melting temperature and satisfactory mechanical properties. However, due to recent legislation and market pressures, Pb is being removed from electronic products [1]. Many lead free solders have been studied as replacements for Sn-Pb solders, and among them Sn-3.5Ag, Sn-0.7Cu and Sn-3.8Ag-0.7Cu solders are the most promising candidates owing to their overall properties, including mechanical properties, wettability, reflow properties and reliability [references…]. However, the properties of these lead free alloys in corrosive environments has not been widely reported, though it is of importance in many automotive, aerospace, maritime and defence applications. This paper presents the results of an experimental programme to investigate the corrosion properties of Sn-Ag-Cu alloys in relation to Sn-Pb alloys.

Fig. 1 shows the schematic structure of solder joints in a flip chip package, in which solder is used to connect the pads on the chip and the Print Circuit Board (PCB). The material for the pads on chip is normally Cu or Al, and Under Bump Metallisations (UBMs) are deposited on top of the pads to increase the wettability and/or act as a diffusion barrier. The material for the pads on PCB is normally Cu, and for the same functions of UBM these pads can have different surface finishes, such as immersion Au, immersion Ag and electroless Ni immersion Au etc. In flip chip packaging, underfill materials are used to fill the gap between chip and PCB, such that the mechanical properties and reliability of the package are increased and the solder joints are protected from working environments; however, the underfill materials still absorb moisture and corrosion media and cause the corrosion of solders. For some other electronic packaging

methods, e.g. wire bonding, solders will be exposed directly to corrosion media, such as air, moisture, air pollutants from industry and oceanic environments, depending on their application. In order to have a high reliability, solder materials must be resistant to such corrosion media. Although currently corrosion of solder alloys is not a major problem for electronic devices used in normal environment, it may be a problem when they are used in a harsh environment, such as oceanic environments. In addition, any halide-containing contamination acquired during assembly, such as from conventional soldering fluxes, may also degrade the corrosion resistance of solder joints [2].

The potentiodynamic polarisation test has been widely used to study the corrosion properties of materials through polarisation curves [4-8]. During potentiodynamic polarisation tests, the sample (working electrode) is scanned from a cathodic polarisation state, and after reaching the corrosion potential (E_{corr}) it begins anodic polarisation. When the sample reaches the passivation potential, if possible a passivation film begins to form on the surface and the current density at this point is called the critical current density (I_{crit}). After this point the corrosion current density begins to drop to a much lower value. When a compact passivation film is formed on the surface, the corrosion current density becomes stable and this current density is called the passivation current density (I_p). After this point the corrosion remains at the same level and the potential of the sample will increase continually until the potential reaches the breakdown potential. At this point the passivation film begins to break and pitting corrosion happens to the material underneath, resulting in an increase of the corrosion current density.

Some researchers have studied the corrosion behaviour of Sn-Zn-X solders [3, 8], Sn-In-Ag solder [9] and Sn-Zn-Ag-Al-XGa [10], but few [11, 12]have studied the corrosion properties of Sn-Ag, Sn-Cu and Sn-Ag-Cu solders.

In this research, 3.5wt.% NaCl solution was used to simulate sea water, and the corrosion properties of Sn-3.5Ag, Sn-0.7Cu and Sn-3.8Ag-0.7Cu solders in this solution were studied through potentiodynamic polarisation tests and compared with that of eutectic Sn-Pb solder. The results may be used as a guideline for choosing solder materials for electronic used in oceanic environments when the previous used Sn-Pb solder has to be replaced by a lead free one.

2. Experimental procedures

In order to test the corrosion resistance of solder materials, a potentiodynamic polarisation test was conducted to obtain polarisation curves using an AutoTafel potentiostat (ACM Instruments, UK). The solders used in the corrosion tests were Sn-3.8Ag-0.7Cu, Sn-3.5Ag and Sn-0.7Cu lead free bulk materials with a eutectic Sn-Pb bulk solder used as a reference. The corrosion media used was 3.5wt.% NaCl solution, which was used to simulate sea water. After the solder materials were cut into blocks (about 10 mm x 10 mm x 10 mm), copper wires with a plastic insulating layer were soldered to them at the opposite face of the blocks to the working surface, and then the samples were mounted with SAMPL-KWICK (Buehler Ltd, UK) mounting material. The samples were polished up to SiC paper grit 1200 and then washed with deionised water and cleaned with methanol. The exposed area of solders was about 100 mm^2. The test cell consisted of the solder material as a working electrode, a platinum foil as a

counter electrode and a saturated calomel electrode (SCE) as a reference electrode with a Luggin capillary bridge connected to the test solution. The distance between the working electrode and the counter electrode was about 35-40 mm. Some samples were tested from -2000 to 4000 mV to determine the necessary scanning range, and based on this all potentiodynamic polarisation experiments were conducted from -800 to 2500 mV at room temperature. Prior to polarisation scanning, the samples were cathodically treated at -1000 mV for 5 min in 3.5wt.% NaCl solution for conditioning. Different scanning rates (from 30mV/min to 300 mV/min) were used to study their influence on the corrosion process. At least three samples were tested for each testing condition.

The microstructure and composition of the corrosion products were analysed by field emission gun scanning electron microscopy (FEGSEM) with energy dispersive analysis of X-ray (EDX) and X-ray diffraction (XRD) was used to identify the corrosion products from the different solder materials after the potentiodynamic polarisation tests.

3. Results

3.1. Potentiodynamic polarisation curves

Fig. 2 shows the potentiodynamic polarisation curves of Sn-Ag solder in 3.5wt.% NaCl solution with different scanning rates. When the scanning rate was 30 mV/min, the corrosion potential (E_{corr}) and passivation current density (I_p) were -705 mV and 0.49 mA/cm^2, respectively; when the scanning rate was 60 mV/min, the corrosion potential and passivation current density were -750 mV and 1.58 mA/cm^2 respectively, and when the scanning rate was 300 mV/min the samples could not reach a stable passivation

stage. Figs. 3 to 5 show the potentiodynamic polarisation curves of Sn-Ag-Cu, Sn-Cu and Sn-Pb solders in 3.5wt.% NaCl solution with different scanning rates, respectively. The curves are similar to those of Sn-Ag solder. For higher scanning rates, the solders have more negative corrosion potentials and higher corrosion current densities (I_{corr}) and passivation current densities, and when the scanning rate is 300 mV/min, the solders cannot have a stable passivation stage. The corrosion current densities of solders were calculated through the Tafel method and summarised together with other corrosion parameters in Table 1.

The corrosion of a material consists of several processes, such as mass transport and electromigration, and normally the overall reaction rate is controlled by one of these processes. In order to get steady-state polarisation curves, the scanning rate for potentiodynamic polarisation tests need to be sufficiently slow. From Figs. 2 to 5, it can be seen when the scanning rate was 30 mV/min and 60 mV/min the polarisation curves were quite close. It seems that for these testing regimes, when the scanning rate was 30 mV/min, the corrosion of solders was close to a steady state.

3.2. Microstructures of corrosion products

Figs. 6 shows the microstructures of corrosion products on different solder materials after the potentiodynamic polarisation tests. The results show that the corrosion products of Sn-3.8Ag-0.7Cu, Sn-3.5Ag, Sn-0.7Cu and Sn-37Pb had similar microstructures. The corrosion products had a platelet-like shape and were loosely distributed on the surface with different orientations. The results also show that when the tests were conducted with a lower scanning rate, the size of the corrosion products

was larger and the corrosion products for lead free solders were larger than those for Sn-Pb solder.

4. Discussion

Abtew et al. [13] provide a brief review of the corrosion properties of lead free solders in microelectronics. Depending on the application and the in-service environment, electronic components may be exposed to corrosion media.

Figs. 7 and 8 show the comparisons of polarisation curves of Sn-Pb and lead free solders when the scanning rate are 30 and 60 mV/min respectively. From these curves and Table 1, it can be seen that Sn-Ag-Cu has the most negative corrosion potential and Sn-Pb has the highest corrosion potential and that, Sn-Ag has a lower corrosion current density than Sn-Pb, Sn-Ag-Cu and Sn-Cu. During the anodic polarisation process, a stable passivation film formed on Sn-Pb and all lead free solders, which can protect the solders and increase their corrosion resistance. Table 1 shows lead free solders have a lower passivation current density and a larger passivation domain (a potential range in which solder is in a stable passivation state) than Sn-Pb solder. Consequently, when passivation films form on the surface of solder materials the films on the lead free solders are more stable than those on Sn-Pb solder and the corrosion rates of lead free solders are slower than that of Sn-Pb solder. It can also be seen that after the passivation film breaks down, the corrosion current density of lead free solders is smaller than that of Sn-Pb solder. Together, these results indicate that the lead free solders have a better corrosion resistance than Sn-Pb in 3.5wt.% NaCl solution. The results also show that the three lead free solder have similar corrosion resistance, but that of Sn-Ag solder is

somewhat better than that of Sn-Cu and Sn-Ag-Cu, due to the lower corrosion and passivation current densities and a larger passivation domain.

The differences in corrosion resistance among these solders can be explained by the structures of the corrosion products. Fig. 9 shows the cross-sections of solders after tests with scanning rate of 30 mV/min. The cross-section microstructure of Sn-Cu solder after polarisation test was similar to that of Sn-Ag-Cu and such that not presented. Figs. 10 and 11 show the element mapping along the cross sections of Sn-Ag-Cu and Sn-Pb solders. Table 2 and 3 show the surface and cross section element concentrations of solder corrosion products from EDX. It can be seen that the corrosion products of Sn-Pb and lead free solders have different structures. For lead free solders, the corrosion products look like having two layers, but actually they have similar compositions and are both Sn- and Cl-rich. For Sn-Ag-Cu and Sn-Ag solders, there are some small Ag-rich white phases distributed among the Sn-rich phases. The results show that the inner layer of the corrosion products for Sn-Ag-Cu and Sn-Cu contains a tiny amount of Cu and the inner layer of corrosion products for Sn-Ag contains slightly more Ag. However, for Sn-Pb solder, the corrosion products have a two-layered structure (Fig. 9c and d), and EDX analysis showed that the outer layer was Sn-rich and the inner layer was Pb-rich. The Pb-rich layer is looser than the Sn-rich layer, and the adhesion strength between these two layers is weak. During corrosion, some of the Sn-rich layer was lifted away from the Pb-rich layer, as shown in Fig. 9c, which may have been caused by a compressive stress formed in the Sn-rich layer due to an increase in volume compared with the original solder. This layer could subsequently break (Fig. 9d) and leave the Pb-rich layer exposed in the corrosion environment. In this case, the corrosion products on the surface of Sn-Pb solder would no longer protect the underlying solder and the

corrosion media may then penetrate into the loose Pb-rich layer and contact with the Sn-Pb substrate, resulting in the Sn-Pb solder having poorer corrosion resistance than lead free solders. For lead free solders, the Sn-rich layer on Sn-Ag solder was more compact than that on Sn-Ag-Cu and Sn-Cu solders, and as a result Sn-Ag solder had a better corrosion resistance than Sn-Ag-Cu and Sn-Cu.

According to potential-pH diagrams, the study of House and Kelsall [14] showed that the corrosion products of Sn in NaCl solution at a given positive potential were SnO_2 and $Sn(OH)_4$. Lin and Mohanty et al. [3,8,10] studied the corrosion properties of Sn-Zn-X and Sn-Zn-Ag-Al-XGa in NaCl solution, and their results showed that the corrosion product on the surface could be SnO, SnO_2, $SnCl_2$ and ZnO etc. depending on the applied potential. In this study, in order to understand the reactions during the corrosion processes, XRD was used to analyse the corrosion products on the surface after the potentiodynamic polarisation tests. Fig. 12 shows the XRD analyses of the corrosion products on the surface of lead free and Sn-Pb solders after the potentiodynamic polarisation tests with the scanning rate of 300 mV/min. The result shows that all the lead free and Sn-Pb solder materials had the same corrosion product, $Sn_3O(OH)_2Cl_2$, which is a complex oxide chloride hydroxide of tin. This corrosion product is consistent with the results from Yu et al. [15] when they studied the corrosion properties of Sn-9Zn and Sn-8Zn-3Bi. The XRD analysis for the corrosion products on the surface of solder materials after the potentiodynamic polarisation test with the scanning rate 30 mV/min showed that they had the same corrosion products as solders after tests with the scanning rate of 300 mV/min. The EDX analysis for oxygen is not accurate due to the technique limit, however, from Table 2 and 3 it can be seen that the Sn/Cl ratio from both EDX surface and cross-section analyses is consistent with that from XRD analysis.

This further confirms that the corrosion product on the Sn-Pb and lead free solders is $Sn_3O(OH)_2Cl_2$.

During the potentiodynamic polarisation test, the initial reaction on the cathode in the neutral solution was oxygen reduction:

$$O_2 + 4e^- + 2H_2O \rightarrow 4OH^- \quad (1)$$

When the current density reached about 10 mA/cm^2, many hydrogen bubbles evolved from cathode, which was caused by the hydrogen evolution on cathode:

$$2H_2O + 2e^- \rightarrow H_2 + 2OH^- \quad (2)$$

The reactions on the anode are quite complicated. Some possible anodic reactions were reported in the literatures [10,16], including:

$$Sn + 2OH^- - 2e^- = Sn(OH)_2 \quad (3)$$

$$Sn + 2OH^- - 2e^- = SnO + H_2O \quad (4)$$

$$Sn(OH)_2 + 2OH^- - 2e^- = Sn(OH)_4 \quad (5)$$

$$SnO + H_2O + 2OH^- - 2e^- = Sn(OH)_4 \quad (6)$$

The dehydration of $Sn(OH)_2$ and $Sn(OH)_4$ into SnO and SnO_2 respectively was also reported [10,16]:

$$Sn(OH)_2 = SnO + H_2O \quad (7)$$

$$Sn(OH)_4 = SnO_2 + 2H_2O \quad (8)$$

However, since in this research only one main corrosion product, $Sn_3O(OH)_2Cl_2$, was found on the surface of Sn-Pb and lead free solders, the reactions above look not possible. In this case, the anodic reaction could be:

$$3Sn + 4OH^- + 2Cl^- - 6e^- = Sn_3O(OH)_2Cl_2 + H_2O \quad (9)$$

Apart from the reactions with Sn, there were also reactions with other elements. As shown in Fig. 9, for Sn-Pb solder, the reactions with Pb formed a loose Pb-rich layer beneath Sn-rich layer, which was detrimental to the corrosion resistance, and for Sn-Ag and Sn-Ag-Cu solders, the reactions with Ag formed some Ag-rich phases among Sn-rich phases. The corrosion product of Pb in sea water could be $PbCl_2$, $PbCO_3 \cdot PbCl_2$, $Pb_3(CO_3)_2(OH)_2$, PbO and Pb_2O_3 [17]. However, in this research, there is no CO_3^{2-} in the solution, so the possible composition of Pb-rich layer could be $PbCl_2$, PbO and Pb_2O_3.

5. Conclusions

The corrosion resistance of lead free and Sn-Pb solders were studied through potentiodynamic polarisation tests and following conclusions can be drawn:

1. Lead free solders exhibit better corrosion resistance than Sn-Pb solder in 3.5wt.% NaCl solution, due to the lower passivation current density, lower corrosion current density after the breakdown of passivation film and a more stable passivation film on the surface. Corrosion resistance of Sn-Ag-Cu, Sn-Cu and Sn-Ag was similar, but that of Sn-3.5Ag was better than that of two others.
2. The corrosion product on the surface of all solders studied after potentiodynamic polarisation tests in 3.5wt.% NaCl solution with different scanning rates was tin oxide chloride hydroxide ($Sn_3O(OH)_2Cl_2$), which had a platelet-like shape and were loosely distributed on the surface with different orientations.
3. The corrosion products on Sn-Pb solder had a two-layered structure with relatively compact Sn-rich phases at the outer layer and loose Pb-rich phases at

the inner layer. The existence of the Pb-rich layer was detrimental to corrosion resistance.

Acknowledgements

The authors acknowledge the financial support for this work under the Engineering and Physical Sciences Research Council Innovative Manufacturing and Construction Research Centre at Loughborough University under contact No. GR/R64483/01P. The authors also wish to acknowledge Dr. Keming Chen for assistance in the potentiodynamic polarisation tests.

References

[1] Directive of the European Commission for the Reduction of Hazardous Substances, Directive 2000/0159 (COD) C5-0487/2002, LEX 391, PE-CONS 3662/2/02 Rev 2, ENV581, CODEC 1273, 2003.

[2] J. Glazer, Metallurgy of Low-Temperature Pb-Free Solders for Electronic Assembly, Int. Mater. Rev. 40 (1995) 65-93.

[3] K.L. Lin, T.P. Liu, The electrochemical corrosion behaviour of Pb-free Al-Zn-Sn solders in NaCl solution, Mater. Chem. Phys. 56 (1998) 171-176.

[4] W.J. Chou, G.P. Yu, J.H. Huang, Corrosion resistance of ZrN films on AISI 304 stainless steel substrate, Surf. Coat. Technol. 167(2003) 59-67.

[5] G. Quartarone, T. Bellomi, A. Zingales, Inhibition of copper corrosion by isatin in aerated 0.5 M H2SO4, Corros. Sci. 45 (2003) 715-733.

[6] J.J. Park, S.I. Pyun, Pit formation and growth of alloy 600 in Cl- ion-containing thiosulphate solution at temperatures 298-573 K using fractal geometry, Corros. Sci. 45 (2003) 995-1010.

[7] Y. Zuo, P.H. Zhao, J.M. Zhao, The influences of sealing methods on corrosion behavior of anodized aluminum alloys in NaCl solutions, Surf. Coat. Technol. 166 (2003) 237-242.

[8] K.L. Lin, F.C. Chung, T.P. Liu, The potentiodynamic polarisation behavior of Pb-free XIn-9(5Al- Zn)-YSn solders, Mater. Chem. Phys. 53 (1998) 55-59.

[9] H. Oulfajrite, et al., Electrochemical behavior of a new solder material (Sn-In-Ag), Mater. Lett. 57 (2003) 4368-4371.

[10] U.S. Mohanty, K.L. Lin, The effect of alloying element gallium on the polarisation characteristics of Pb-free Sn-Zn-Ag-Al-XGa solders in NaCl solution, Corros. Sci. 48 (2006) 662-678.

[11] D.Q. Yu, W. Jillek, and E. Schmitt, Electrochemical migration of Sn-Pb and lead free solder alloys under distilled water, J. Mater. Sci. - Mater. Electron. **17** (2006) 219-227.

[12] B.Y. Wu et al., Electrochemical corrosion study of Pb-free solders. J. Mater. Res. **21**(2006) 62-70.

[13] M. Abtew, G. Selvaduray, Lead-free solders in microelectronics, Mater. Sci. and Eng. R 27 (2000) 95-141.

[14] C.I. House, G.H. Kelsall, Potential-pH diagrams for the Sn/H_2O-Cl system, Electrochim. Acta 29 (1984) 1459-1464.

[15] D.Q. Yu, C.M.L. Wu, L. Wang, The electrochemical corrosion behavior of Sn9Zn and Sn-8Zn-3Bi lead-free solder alloys in NaCl solution, 16th International corrosion conference, Beijing, China, 2005, 19-24.

[16] S.D. Kapusta and N. Hackerman, Anodic passivation of tin in slightly alkaline solutions, Electrochim. Acta **25** (1980) 1625-1639.

[17] A.M. Beccaria, E.D. Mor, G. Bruno, G. Poggi, Investigation on lead corrosion products in sea water and in neutral saline solutions, Mater. Corr. 33 (1982) 416-420.

Lists of table and figure captions

Fig. 11. Element mapping for cross-section of Sn-Pb solders after potentiodynamic polarization test with scanning rate at 30 mV/min.

Fig. 12. XRD spectra of different solder materials after the corrosion tests with the scanning rate at 300 mV/min.

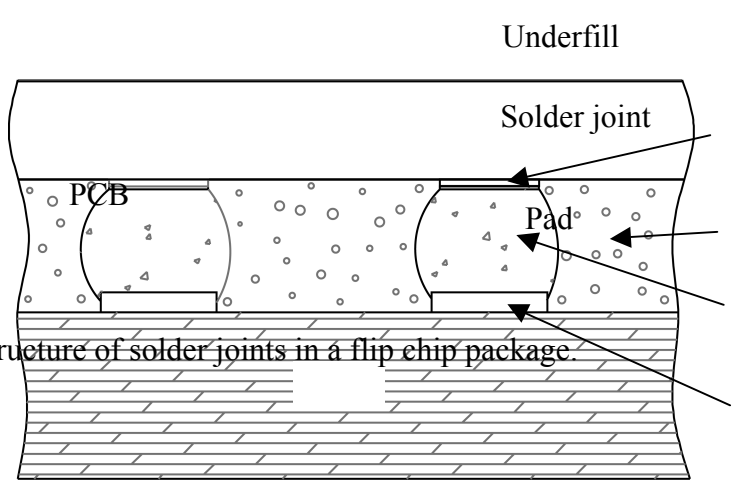

Fig. 1. Schematic structure of solder joints in a flip chip package.

Fig. 2. Potentiodynamic polarization curves of Sn-Ag solder in 3.5 wt.% NaCl solution.

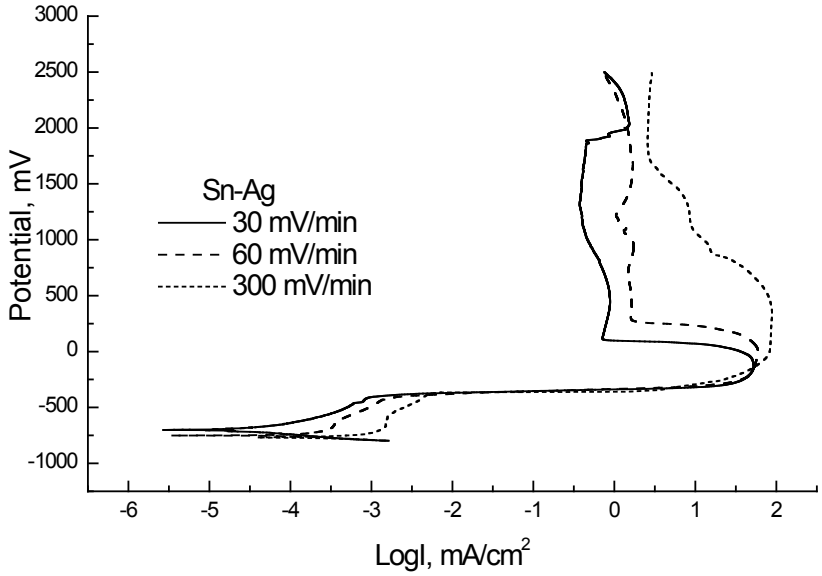

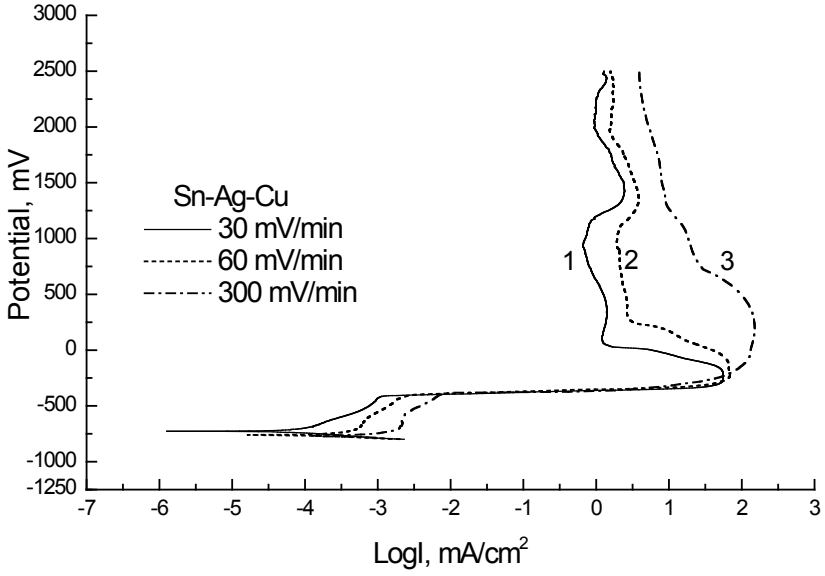

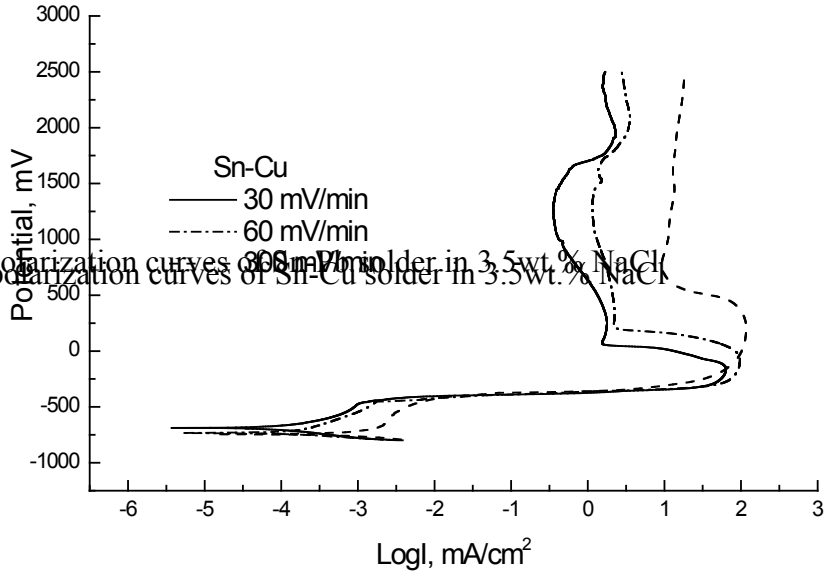

Fig. 4. Potentiodynamic polarization curves of Sn-Cu solder in 3.5wt.% NaCl solution.

Fig. 5. Potentiodynamic polarization curves of Sn-Pb solder in 3.5wt.% NaCl solution.

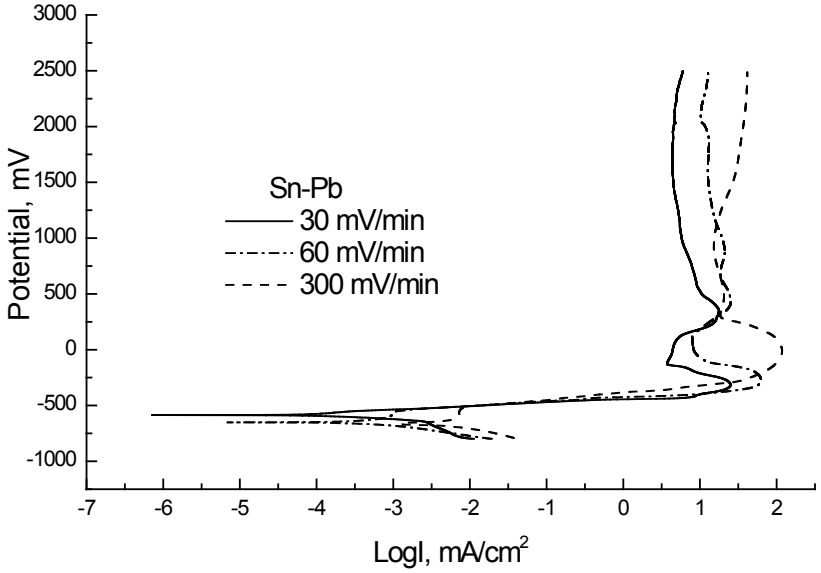

a b

c

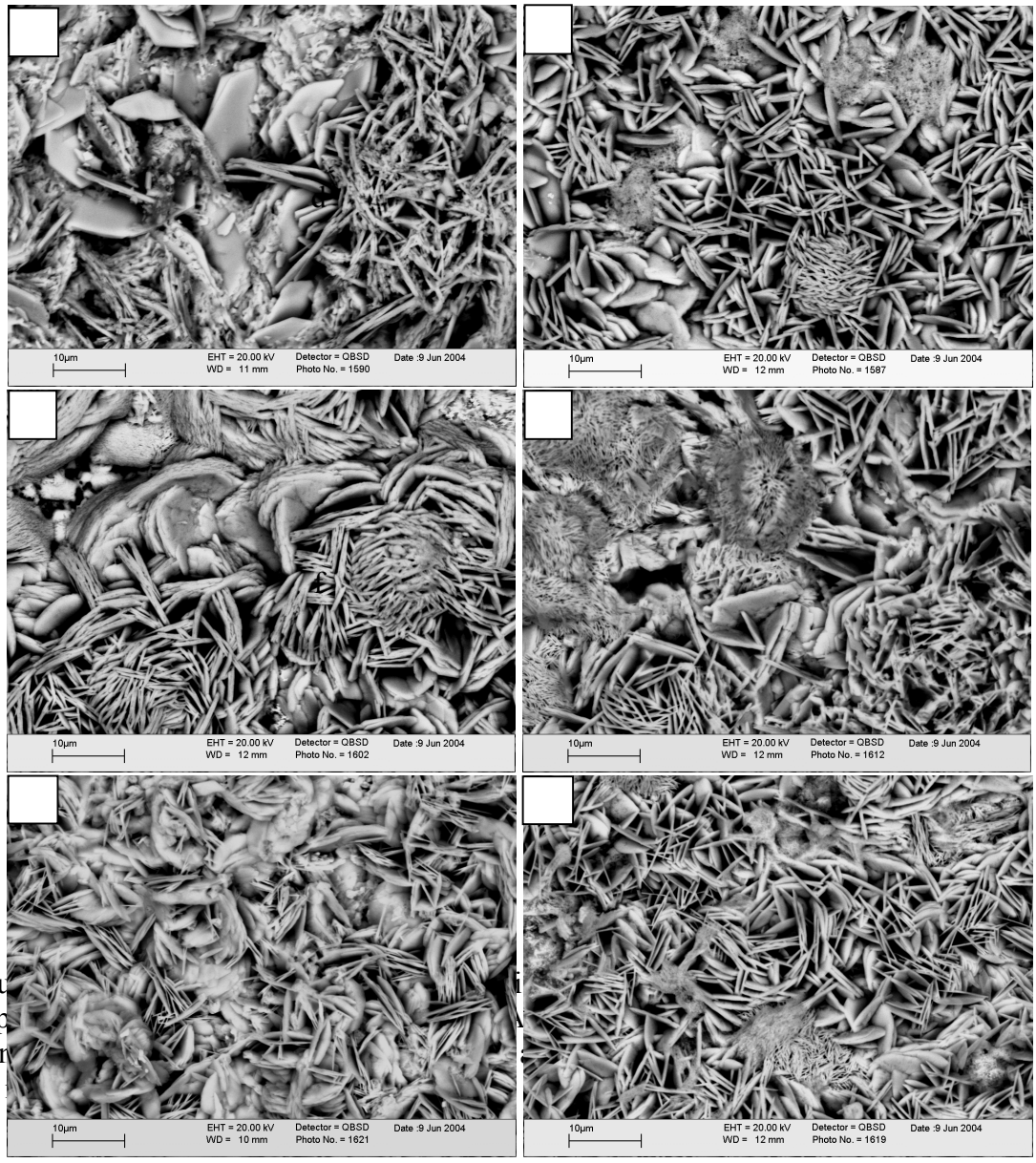

e

Fig. 6. Microstru
potentiodynamic p
Sn-Pb; the scannir
for a) and e) is 30

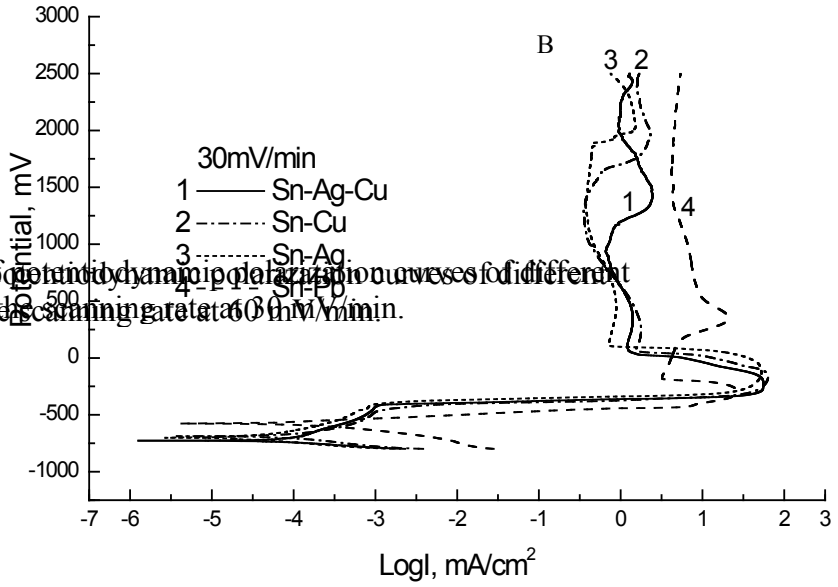

Fig.8.7 Comparison of potentiodynamic polarization curves of different solder materials with the scanning rate at 60 mV/min.

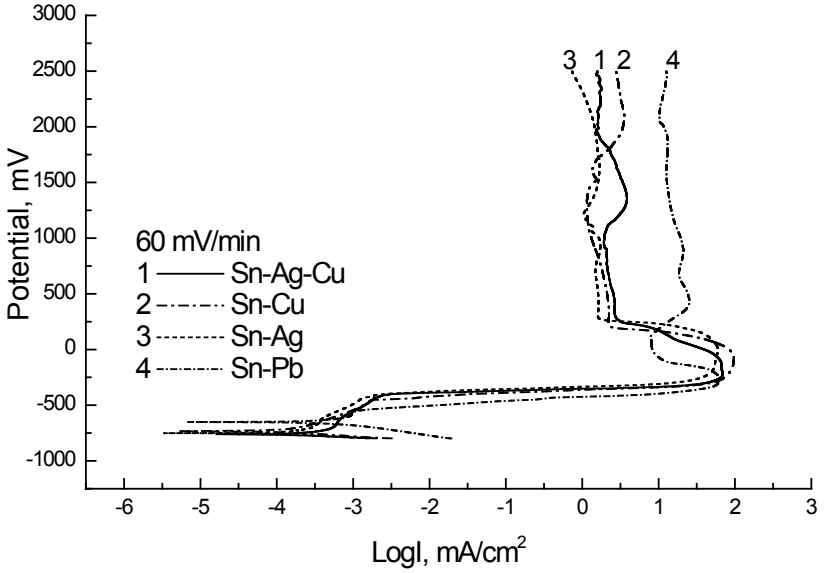

a b

c d

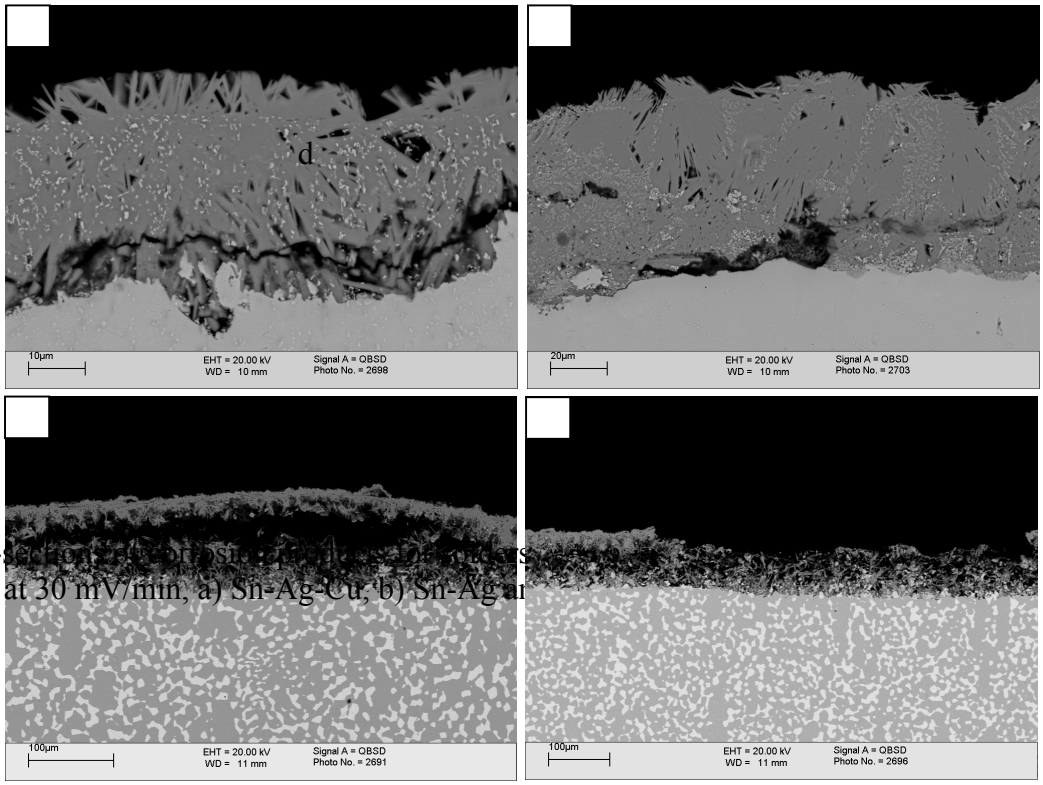

Fig. 9. Cross-sectional morphologies of solders [illegible] scanning rate at 30 mV/min, a) Sn-Ag-Cu, b) Sn-Ag a[illegible]

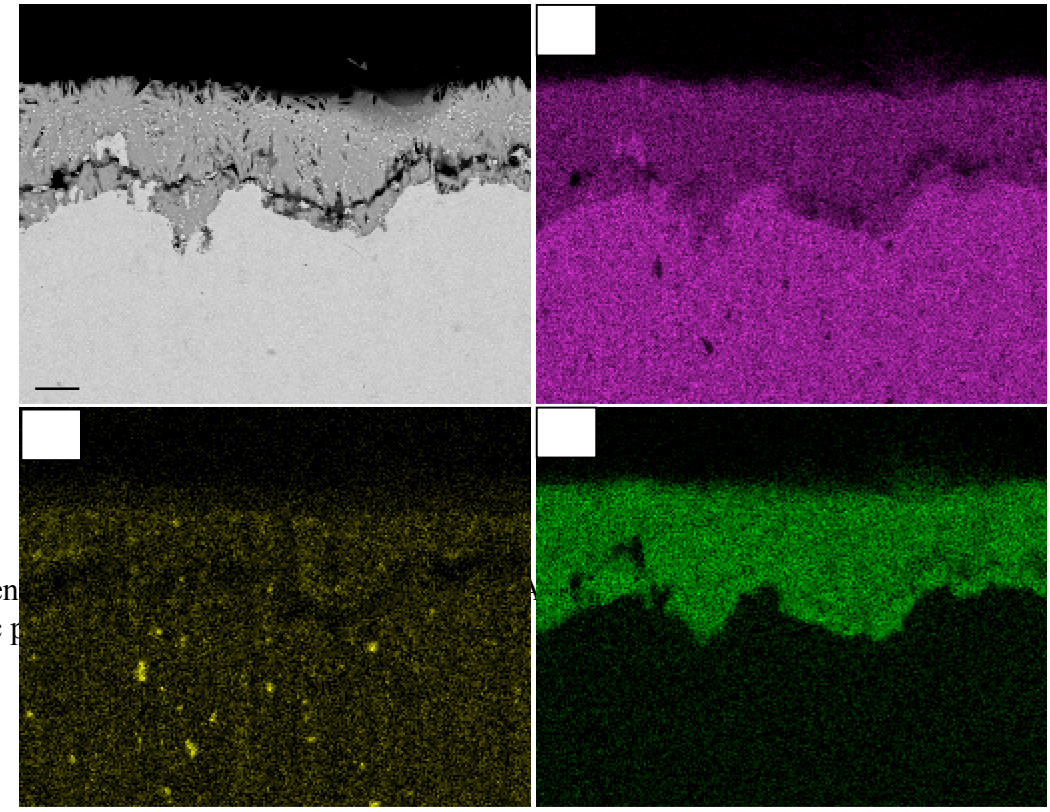

Fig. 10. Elemen A potentiodynamic p

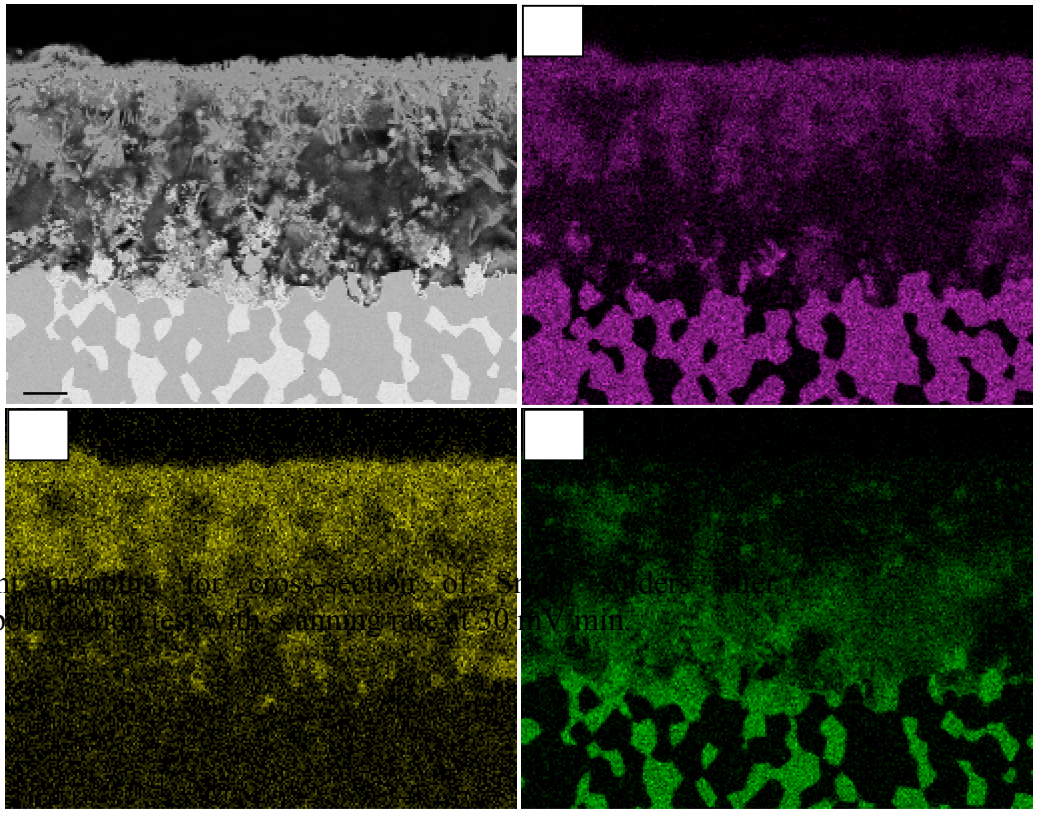

Fig. 11. Elemen mapping for cross-section of Sn der under potentiodynamic p rization curves) with scanning rate at 30 mV/min.

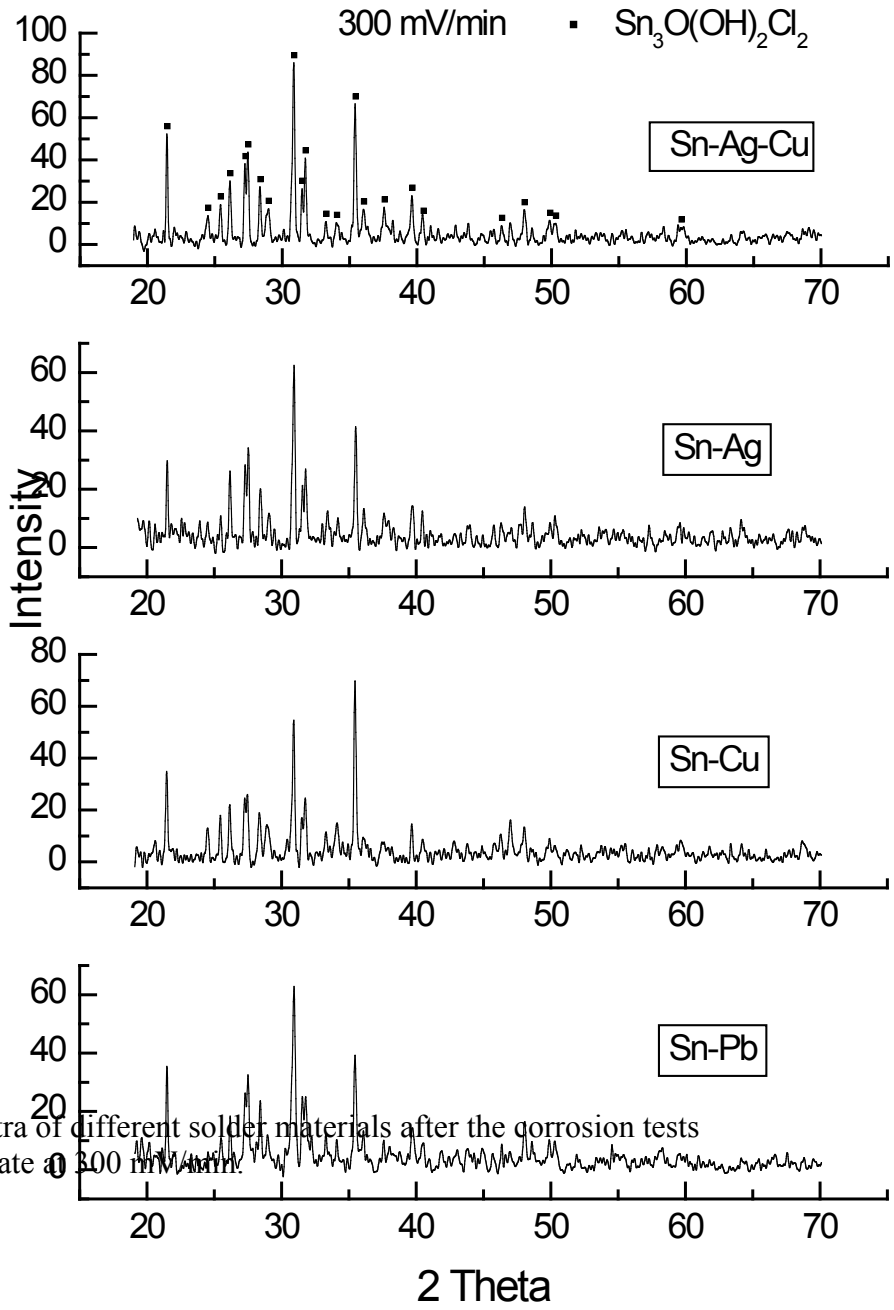

Fig. 12. XRD spectra of different solder materials after the corrosion tests with the scanning rate at 300 mV/min.

Table 3. Cross-section element concentration of different solders after potentiodynamic polarisation tests with scanning rate at 30 mV/min.

Scanning rate	E_{corr} (mV)	I_p (mA/cm^2)	I_{corr} (μA/cm^2)	I_{crit} (mA/cm^2)	D_p (mV)
Sn-Ag-Cu					
30	-727	1.07	0.089	54.95	1089
60	-763	2.24	0.288	70.79	797
300	-772	-	0.617	151.36	-
Sn-Cu					
30	-688	0.74	0.178	66.07	1560
60	-735	1.62	0.166	100.0	1442
300	-744	9.2	0.661	120.23	-
Sn-Ag					
30	-705	0.49	0.048	50.12	1766
60	-750	1.58	0.155	63.10	927
300	-771	-	0.708	112.20	-
Sn-Pb					
30	-576	4.17	0.074	26.30	368
60	-653	8.1	0.525	64.57	265
300	-723	16.5	1.905	114.82	-

E_{corr} – corrosion potential, I_p – passivation current density, I_{corr} – corrosion current density, I_{crit} – critical passivation density and D_p – passivation domain.

	Surface element concentration (At %)			
	Sn	Ag	Cl	O
Sn-Ag	43.34	5.44	29.09	22.13
Sn-Cu	47.22	-	34.56	18.22
Sn-Ag-Cu	48.36	-	32.58	19.06
Sn-Pb	46.37	-	32.74	20.89

		Cross-section element concentration (At %)				
		Sn	Ag	Cl	Pb	Cu
Sn-Ag	-	57.48	2.0	40.52	-	-
Sn-Cu	Top layer	59.72	-	40.28	-	-
	Inner layer	56.26	-	40.96	-	2.78
Sn-Ag-Cu	Top layer	59.59	-	40.41	-	-
	Inner layer	55.5	-	41.8	-	2.69
Sn-Pb	Top layer	57.75	-	42.25	-	-
	Inner layer	32.38	-	39.01	28.61	-